2.2 The Use of Potential Vorticity in Tropical Dynamics

Wayne H. Schubert*

1. Introduction

For a nonhydrostatic, moist, precipitating atmosphere, the appropriate generalization of the well-known (dry) Ertel potential vorticity principle is

$$\frac{DP}{Dt} = \frac{1}{\rho}(\nabla \times \mathbf{F}) \cdot \nabla\theta_\rho + \frac{1}{\rho}\boldsymbol{\zeta} \cdot \nabla\dot{\theta}_\rho, \qquad (1)$$

where

$$P = \frac{1}{\rho}\boldsymbol{\zeta} \cdot \nabla\theta_\rho \qquad (2)$$

is the potential vorticity, $\boldsymbol{\zeta} = 2\boldsymbol{\Omega} + \nabla \times \mathbf{u}$ the absolute vorticity, ρ the total density, consisting of the sum of the densities of dry air, airborne moisture (vapor and cloud condensate) and precipitation, $\mathbf{u}$ is the velocity of the dry air and airborne moisture, and $\theta_\rho = T_\rho(p_0/p)^{R_a/c_{Pa}}$ is the virtual potential temperature, with $T_\rho = p/(\rho R_a)$ the virtual temperature, p the total pressure (the sum of the partial pressures of dry air and water vapor), p_0 the constant reference pressure, R_a the gas constant for dry air, and c_{Pa} the specific heat at constant pressure for dry air. Since θ_ρ is a function of total density and total pressure only, its use as the thermodynamic variable in P leads to the annihilation of the solenoidal term, i.e., $\nabla\theta_\rho \cdot (\nabla\rho \times \nabla p) = 0$. Equation (1) is a generalization of the well-known (dry) Ertel potential vorticity principle in three respects: (i) ρ is the total density, consisting of the sum of the densities of dry air, water vapor, airborne condensate, and precipitation; (ii) θ_ρ is the virtual potential temperature; (iii) Precipitation effects are included in $\mathbf{F}$. In the special case of an absolutely dry atmosphere, P reduces to the usual (dry) Ertel potential vorticity.

For balanced flows, there exists an invertibility principle which determines the balanced mass and wind fields from the spatial distribution of P. It is the existence of this invertibility principle that makes P such a fundamentally important dynamical variable. In other words, P (in conjunction with the boundary conditions associated with the invertibility principle) carries all the essential dynamical information about the slowly evolving balanced part of the moist, precipitating, atmospheric flow.

In this talk we consider four tropical phenomena that can be better understood using PV dynamics: (1) The emergence of twin tropical cyclones from super cloud clusters which straddle the equator; (2) the formation and breakdown of shear zones associated with ITCZ convection; (3) the flatness of the trade wind inversion; (4) mixing processes, polygonal eyewalls, and rapid pressure falls in hurricanes.

2. Twin tropical cyclones

For simplicity, we now neglect the frictional term in (1) and concentrate on the diabatic source/sink term, which plays a crucial role in many tropical phenomena. This diabatic source/sink term in the PV principle (1) can be rewritten as

$$\begin{aligned}\frac{1}{\rho}\boldsymbol{\zeta} \cdot \nabla\dot{\theta}_\rho &= \frac{1}{\rho}\boldsymbol{\zeta} \cdot \nabla\theta_\rho \left(\frac{\boldsymbol{\zeta} \cdot \nabla\dot{\theta}_\rho}{\boldsymbol{\zeta} \cdot \nabla\theta_\rho}\right) = P\left(\frac{\mathbf{k} \cdot \nabla\dot{\theta}_\rho}{\mathbf{k} \cdot \nabla\theta_\rho}\right) \\ &= P\left(\frac{\partial\dot{\theta}_\rho/\partial Z}{\partial\theta_\rho/\partial Z}\right) = P\frac{\partial\dot{\theta}_\rho}{\partial\Theta_\rho}\end{aligned}$$

where $\mathbf{k} = \boldsymbol{\zeta}/|\boldsymbol{\zeta}|$ is the unit vector along the vorticity vector and $\partial/\partial\Theta_\rho$ denotes the derivative along the vorticity vector. Equation (1) can now be written as

$$\frac{DP}{Dt} = P\frac{\partial\dot{\theta}_\rho}{\partial\Theta_\rho}. \qquad (3)$$

This form emphasizes the exponential nature of the time behavior of P for material parcels. We note two important facts: (i) $P \approx 0$ near the equator, so that diabatic heating near the equator has little effect on PV; (ii) $\dot{\theta}_\rho$ peaks in midtroposphere, so convective clusters are a "material" source of PV in the lower troposphere and a sink in the upper troposphere.

The effect of the P term on the right hand side of (3) can be understood in the simpler context of the shallow water equations. For the inviscid shallow water equations with a mass source/sink term Q on the right hand side of the continuity equation, the PV principle is

$$\frac{DP}{Dt} = P\left(-\frac{Q}{h}\right), \qquad (4)$$

Author address: Department of Atmospheric Science, Colorado State University, Fort Collins, CO 80523-1375; e-mail: waynes@atmos.colostate.edu

where $P = \left(\bar{h}/h\right)\zeta$ is the potential vorticity, with h the fluid depth, $\bar{h}$ the constant initial mean fluid depth, ζ the absolute vorticity, and D/Dt the material derivative in the shallow water system. Because of the similarity of (3) and (4), we now examine some shallow water simulations with mass source/sinks near the equator.

Figs. 1–3 show the temporal evolution of the shallow water fluid depth, the PV, and the winds produced by an elliptically shaped mass sink within the dotted curve. After 2 days of simulation, a Kelvin wave signature dominates the flow to the east of the mass sink. This Kelvin wave part of the solution is essentially invisible on the PV map. In the region of the mass sink, two cyclonic PV anomalies on opposite sides of the equator are being produced through the $-PQ/h$ term in (4). Since this term vanishes at the equator, there is no PV anomaly produced there. Equatorial westerly winds occur in the region of the mass sink and to its west. The geopotential and wind fields at this time are very similar to the linear, steady state results of Gill. The two cyclones and the equatorial westerly winds continue to intensity through day 5. The westerly wind burst depicted in Fig. 3 is exactly on the equator. This should excite an oceanic Kelvin wave which is confined to within just a few degrees latitude about the equator. If the simulated atmospheric convection, outlined by the dotted curve in Fig. 1, is shifted only slightly north or south, the westerly wind burst does not occur on the equator, and an oceanic Kelvin wave would probably not be excited.

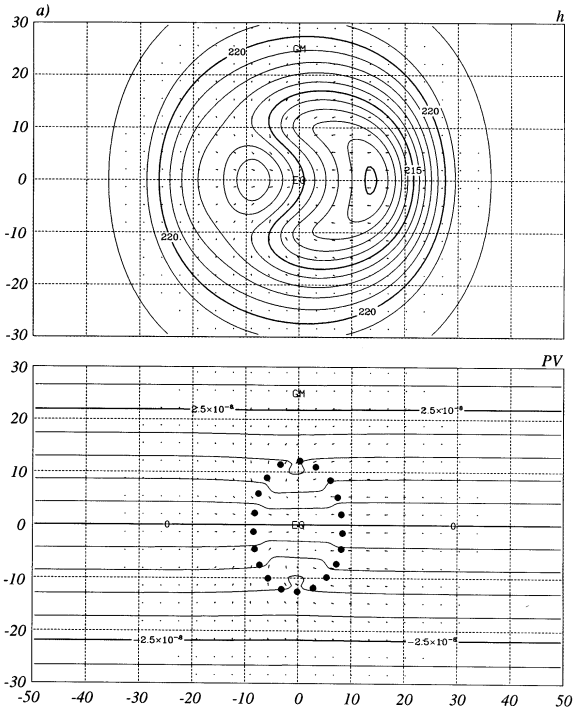

Figure 1: Formation of twin tropical cyclones, day 1.

3. Formation and breakdown of shear zones associated with ITCZ convection

During the northern summer, the ITCZ over the Pacific is zonally elongated and often wider and more active on its western and eastern ends. Fig. 4 shows the evolution of the fluid depth, wind, and PV fields produced by an irregularly shaped mass sink, the outline of which is shown by the dots. A reversal of the poleward gradient of PV first appears during day 2 of the integration, providing the necessary condition for the occurrence of barotropic instability. At 5 days a cyclonic PV strip that is wider on its eastern and western ends has been produced. It is important to also note that the cyclonic PV anomaly is most intense in the poleward half of the mass sink. This is a robust consequence of the P factor on the right hand side of the potential vorticity equation. ITCZ cloud bands produce strips of enhanced PV that are about half the cloud band width. These narrow PV strips are more dynamically active (i.e., have faster growth rates of barotropic instability) than wider ones. Narrow strips also produce "easterly waves" of shorter zonal wavelength. Another interesting feature of Fig. 4 is that, during this barotropic instability process, two plumes of negative PV are drawn across the equator into the northern hemisphere. Associated with these PV anomalies are two regions of trade wind surges in the the southern hemisphere.

4. The flatness of the trade wind inversion

In schematic north-south cross sections the trade inversion layer is often depicted as sloping upward as air flows toward the ITCZ. This conceptual view is consistent with *purely thermodynamic* boundary layer models, which predict a deeper boundary layer with increasing sea-surface temperature and decreasing large-scale subsidence. The slopes implied by such thermodynamic models and incorporated into schematic diagrams are approximately 2000 m/1000 km. In contrast, observational studies of the inversion structure over the Atlantic and Pacific reveal a less dramatic slope, on the order of 300 m/1000 km. This inconsistency can be resolved by adopting a somewhat different view of the trade inversion layer. In particular, rather than regarding it as a purely thermodynamic structure,

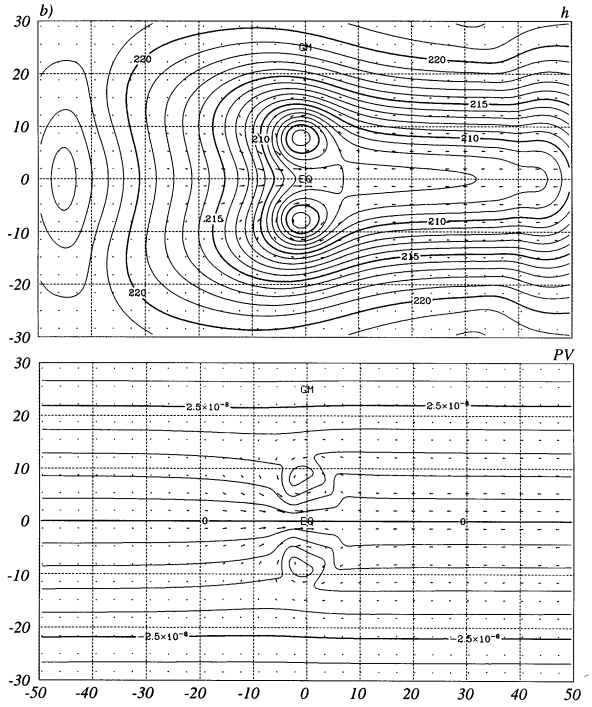

Figure 2: Formation of twin tropical cyclones, day 2.

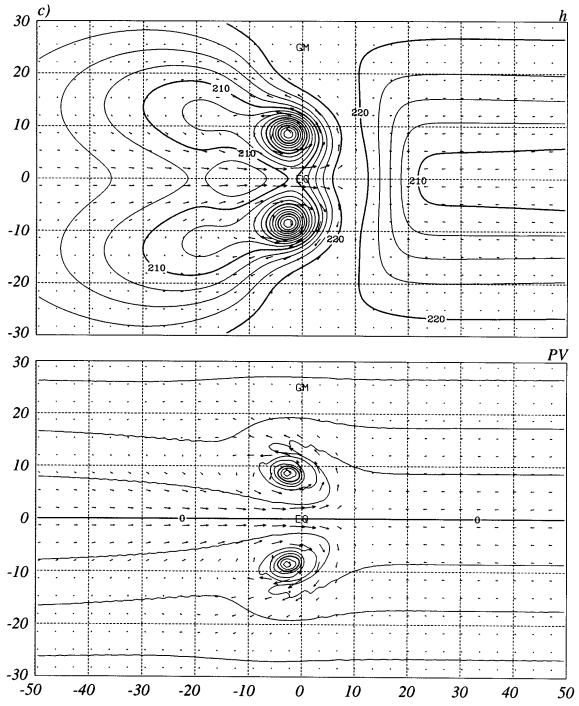

Figure 3: Formation of twin tropical cyclones, day 5.

regard it as a dynamical structure, a thin layer of high potential vorticity. By formulating a generalization of the Rossby adjustment problem, we can investigate the dynamical adjustments of a tradewind inversion layer of variable strength and depth. From the solution of the adjustment problem there emerges the notion that the subtropics control the inversion structure in the tropics, i.e., that the subtropical inversion height is dynamically extended into the tropics in such a way that there is little variation in the depth of the boundary layer.

5. Mixing processes, polygonal eyewalls, and rapid pressure falls in hurricanes

In the intense convective region of a hurricane the absolute vorticity vector tends to point upward and radially outward. Since $\dot{\theta}_\rho$ tends to be a maximum at midtropospheric levels, air parcels flowing inward at low levels and spiraling upward in the convective eyewall experience a material increase in PV due to the $P(\partial\dot{\theta}_\rho/\partial\Theta_\rho)$ term. This material increase of PV can be especially rapid in lower tropospheric regions near the eyewall, where both P and $\partial\dot{\theta}_\rho/\partial\Theta_\rho$ are large. Although the $\partial\dot{\theta}_\rho/\partial\Theta_\rho$ term reverses sign at upper tropospheric levels, large PV is often found there because the large lower tropospheric values of PV are carried upward into the upper troposphere. The resulting spatial structure of the PV field might be expected to be a tower of high PV. Although this conceptual model seems reasonably accurate, it needs some refinement related to the eye region. Once an eye has formed, there is no latent heat release in the central region, and large values of PV would not tend to occur there unless they were transported in from the eyewall. The resulting spatial structure of the PV field might then be expected to be a tower of high PV with a hole in the center or, equivalently, an annular tower of high PV with low PV in the central region. The reversal of the radial PV gradient near the eyewall might also be expected to set the stage for dynamic instability and rearrangement of the PV distribution. If, during the rearrangement process, part of the low PV fluid in the eye is mixed into the eyewall, asymmetric eye contraction can occur in conjunction with a polygonal eyewall. While PV maps of hurricanes are beginning to be constructed from various types of available data, we still need much more observational evidence for the fine scale PV mixing which is likely occurring continuously in the inner core of hurricanes. A tantalizing aspect of the polygonal eyewall phenomenon is that it may be a small window on such PV mixing.

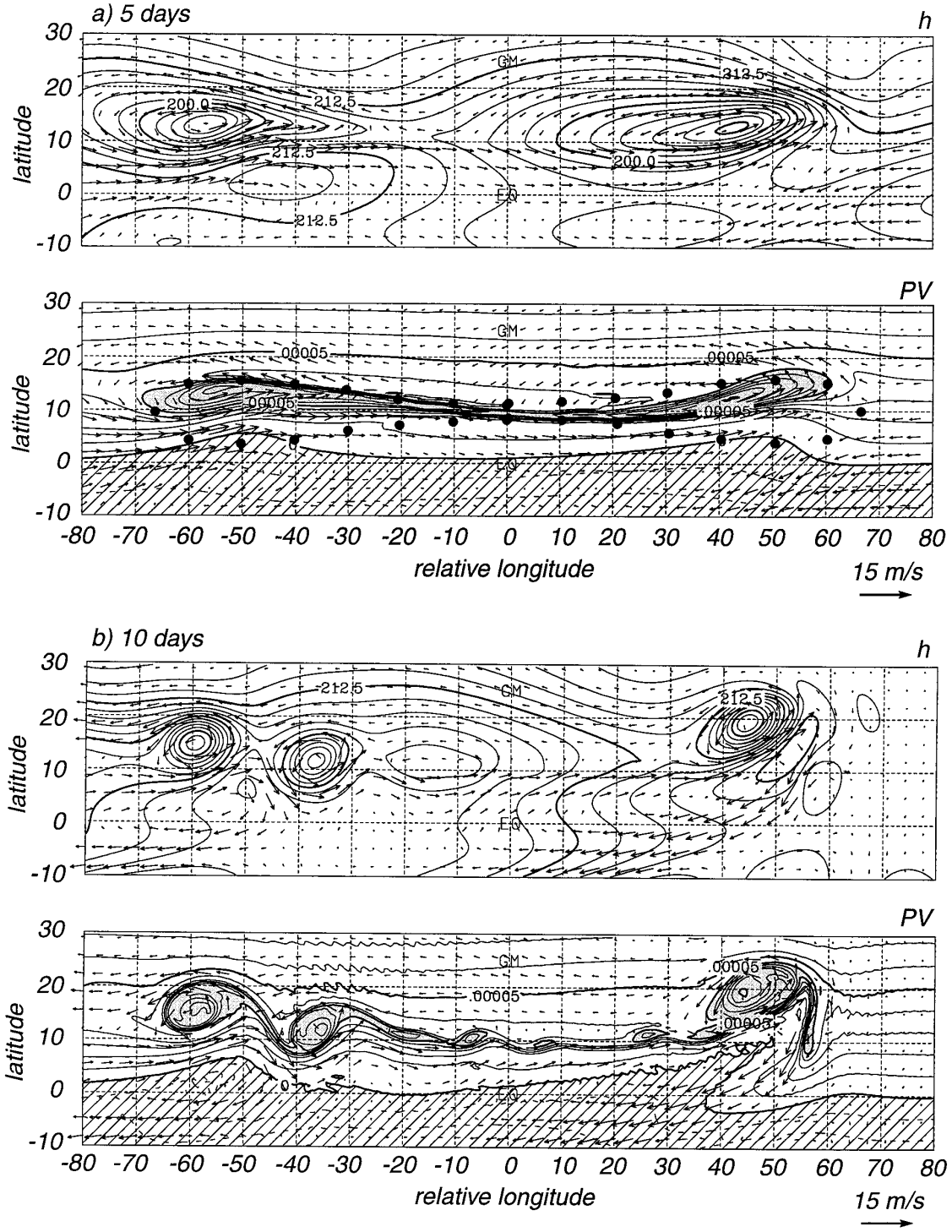

Figure 4: Breakdown of the ITCZ.